



Enhancing asphaltic mixtures with Calcined Nano Montmorillonite: A performance assessment

Amjad H. Albayati^{a,*}, Yu Wang^b, Aliaa F. Al-ani^c

^a Department of Civil Engineering, University of Baghdad, Baghdad 10071, Iraq

^b School of Science, Engineering & Environment, University of Salford, Manchester M5 4WT, UK

^c Department of Civil Engineering, University of Baghdad, Baghdad 10071, Iraq

ARTICLE INFO

Keywords:

Nanoclays
Nano montmorillonite
Calcined Nano Montmorillonite
CT index
Fatigue
Moisture damage
Permanent deformation

ABSTRACT

There are increasing interest in using nanoclay particles to improve asphalt binder and the produced concrete in pavement engineering. However so far most of the study was to directly use the nanoclays in natural material conditions, which come with some inefficient factors affecting the final effectiveness of the modified asphalt binder and the made concrete. This paper reports extensive experimental research on using preprocessed nanoclay, the Calcined Nano Montmorillonite (CNMM), to modify asphalt binder, compared with using natural Nano Montmorillonite (NMM). The nanoclays were added in asphalt as additive at different content rates ranging from 0% to 10% by the weight of asphalt binder. Experimental tests were performed on both of the modified asphalt binders and the concrete mixes using them. The study showed that at a 10% content CNMM demonstrated 32% improvement on Indirect Tensile Strength (ITS), and 5.25% less permanent deformation after exposed 10,000 load repetitions; at 6% CNMM presented 57.5% improvement on the CTindex for fatigue resistance. Meanwhile, the SEM analysis proved a distinctive morphological difference between NMM and CNMM, which indicates the optimized microscopic structure of the CNMM for the improvement on the interlock and adhesion with asphalt binder. In comparison, the optimum dosage for NMM is identified at 4%, while CNMM is at around 6%. The economic viability of the use of CNMM against the use of NMM has also been discussed in reference to the local material prices. In consideration of a balance between cost and performance, 6% content is recommended for the use of CNMM.

1. Introduction

In the ever-evolving field of pavement engineering, the quest for enhancing the performance of asphalt concrete remains the paramount effort. Using mineral additives as asphalt modifier has been widely practiced and proved to be effective [4,17,45,48]. These additives are added in and mixed with asphalt cement at the mixing stage or beforehand, which can improve asphalt concrete properties, particularly for their thermal stability [6,7]. There are increasing interest in research using wider potential materials, such as the use of polymer and wax [10], steel slag [43], for asphalt binder additive and the use recycled gravels for asphalt concrete and pavement aggregates (Azam et al., 2017, [15,38]), in order to not only improve asphalt concrete performance, but also help reduce waste disposal and the cost relying on traditional resource (Walker, 2023, [11,36]).

* Corresponding author.

E-mail address: a.khalil@uobaghdad.edu.iq (A.H. Albayati).

Among the optional additives for asphalt binder improvement, nanoclays have received particularly attention because of their abundant global reservation as well as their advantage in material compositive characterization [1,27,33–35,37,41] [8,40,46]. Research studies have demonstrated that using nanoclays to modify asphalt can enhance the performance of the binders and concrete mixes with increasement on the softening point temperature, viscosity, the dynamic shear complex modulus, and rutting and fatigue resistance, and decrement on penetration value and the strain failure rate [16,33,42,47]. Nanoclays can increase the cohesion of asphalt binder, enhancing the resistance to cracking [23]. In addition, nanoclays can help reduce the moisture sensitivity of asphalt concrete [12,14,21] to improve the aging resistance [26].

Nanoclays are layered silicates [47], which, upon composition and particle morphology, are classified into montmorillonite, bentonite, kaolinite, hectorite, and halloysite. Nanoclay particles are in platelet form of a high width to thickness ratio up to 70–150 [19]. This nature makes nanoclays have high specific surface area and anisotropic characteristic. Mixing nanoclay particles with polymer, polymer molecules will infiltrate into the interstices between layer slices to form a sandwich structure [29] that will largely alter the physical and mechanical properties of the polymer matrix in a form of an exfoliated morphology. You et al., [47]. Taking advantage of this mechanism, nanoclays have been explored as additive to modify asphalt, for which research has been elaborated on the effects of nano-particle type, size, content and production process [31].

Montmorillonite (MMT) is one of the most frequently used nanoclays. It has a 2:1 layered structure with two silica tetrahedron sandwiching an alumina octahedron. As one of the most extensively studied mineral modifiers, MMT showed improvement on the high-temperature properties and aging resistance of bitumen [5,18,20,25,28,30]. When the MMT is added into the asphalt, the molecular chain of the asphalt could be intercalated into the layer structure of MMT, which form an intercalated structure or an exfoliated structure. The hydrogen bonds and van der Waals interactions between MMT and molecular chain of the asphalt hinder the thermal motion of molecular chain of asphalt [22]. The intercalated structure and exfoliated structure can also effectively decrease the permeability of oxygen, slow down the aging of asphalt and improve the durability of asphalt. Ashish et al., [9].

So far, most research on nano clay additives predominantly focused on the application of conventional Nano Montmorillonite (NMM) in asphalt, which contains moisture and organisms. However, using preprocessed nano clay, such as the use of Calcined Nano Montmorillonite (CNMM) in asphalt concrete has little reported in literature. Recognized this gap, this research aims to highlight the potential of CNMM as a promising asphalt additive as the preprocessed nano clay has much lower moisture content, higher purity and other potential unrevealed benefits. This paper reports an experimental investigation to assess effectiveness of the preprocessed nano clay CNMM on the performance properties of asphalt concrete mixtures and compare them with that using conventional NMM. The effects on both the binder and the produced asphalt concrete mixtures were studied. The compared binder properties include penetration, softening point, and compatibility (storage stability). The compared concrete mixture properties include Marshall characteristics, permanent deformation, moisture susceptibility, fatigue resistance, as well as the resilient modulus. At the end, cost analysis was also conducted to assess the economic feasibility between the use of CNMM and NMM.

2. Materials

2.1. Asphalt cement

An asphalt cement of 40–50 penetration grade was employed, which was sourced from the Dora refinery in the southwest of Baghdad. Table 1 lists out its physical properties, which meet the specification for type AC 40/50 by the State Corporation of Roads and Bridges [39].

2.2. Coarse and fine aggregates

The aggregates were crushed quartz, sourced from the Amanat Baghdad, an asphalt concrete mix plant situated in Taji, north of Baghdad. The aggregates were sieved at first into coarse and fine class, and subsequently recombined in term of grade for mix type III A used for wearing course with a nominal maximum aggregate size of 12.5 mm/0.5 in. [39]. Fig. 1 exhibits the gradation curve of the aggregates. Table 2 compares the aggregates' physical properties against the specification, which fall in the range.

Table 1
Properties of asphalt cement.

Test	Unit	ASTM designation	Result	Specification limit[39]
Penetration at 25 °C, 100 gm., and 5 s	0.1 mm	ASTM D5	47	40–50
Softening point, ring and ball.	°C	ASTM D36	54	—
Specific gravity at 25 °C.	—	ASTM D70	1.03	—
Flashpoint.	°C	ASTM D92	291	Min. 232
Ductility.	cm	ASTM D113	130	Min. 100
Residue from thin film oven test (ASTM D1754).				
Retained penetration, % of original.	%	ASTM D5	58	Min. 55
Ductility at 25 °C, 5 cm/min.	cm	ASTM D113	75	Min. 25

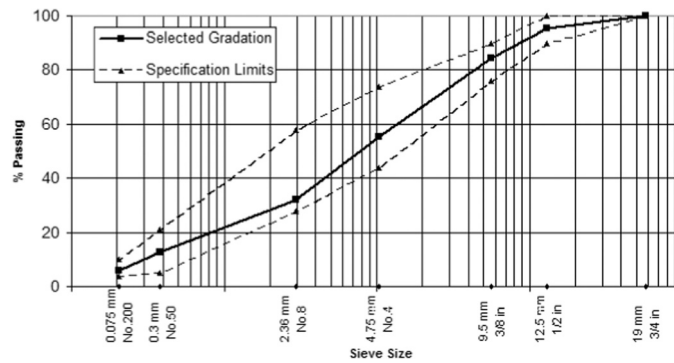


Fig. 1. Aggregate gradation for wearing course and specification limits.

Table 2

Coarse and fine aggregate physical properties.

Test	ASTM designation	Result	Specification of [39]
Coarse Aggregate			
Apparent Specific Gravity	ASTM C127	2.721	-
Bulk Specific Gravity		2.688	-
Water Absorption, (%)		0.324	-
Soundness (Sodium Sulfate Solution Loss), %	ASTM C88	3.4	12 max.
Percent Wear (Los Angeles abrasion), (%)	ASTM C131	17	30 max.
Flat & Elongated (5:1), (%)	ASTM D4791	7	10 max.
Fractured Pieces, (%)	ASTM D5821	94	90 min
Fine Aggregate			
Apparent Specific Gravity	ASTM C128	2.589	-
Bulk Specific Gravity		2.504	-
Water Absorption, (%)		0.922	-
Clay Lump and Friable Particles, (%)	ASTM C142	2.11	3 max.
Sand Equivalent (%)	ASTM D2419	54	45 min

2.3. Limestone filler

Limestone dust was used as a mineral filler, which was sourced from the lime factory in Karbala governorate, southwest of Baghdad. Table 3 lists out its chemical composition and physical properties.

2.4. Asphalt cement modifiers

Two types of asphalt modifiers were investigated in this study, they were nano montmorillonite (NMM), produced from a montmorillonite clay supplied by Iraqi state company for geological survey and mining, and thermally treated or Calcined Nano Montmorillonite (CNMM), which was produced by heating the NMM in a furnace of 700 °C for a duration of 2 h to eradicate the inherent plasticity and swelling characteristics of the montmorillonite clay. The chemical composition and physical properties of the both types of MM are presented in Table 4.

Fig. 2 compares visually the exterior morphology, crystalline structure and particles size for the NMM and CNMM on the scanning electron microscope (SEM) images at a magnification level of 20k. It shows that the NMM has bigger average particle size. The particles possess a smoother surface and a distinct layered pattern. The CNMM particles are much smaller in size, which exhibit a more disrupted or fragmented form and a rougher or more irregular surface texture due to the loss of the interlayer water and some organic components after the heating process.

Table 3

Chemical composition and physical properties of the filler.

Chemical Composition, %							
CaO	SiO ₂	Al ₂ O ₃	MgO		Fe ₂ O ₃	SO ₃	L.O.I
64.2	8.46	1.9	0.37	0.42		0.81	23.84
Physical Properties							
Specific Gravity	Surface Area* (m ² /kg)				Passing Sieve No. 200 (0.075), %		
2.79	236				98		

* Blain air permeability technique (ASTM C204)

Table 4
Properties of modifiers.

Modifier type	Chemical Composition, %								Physical Properties		
	SiO ₂	CaO	Al ₂ O ₃	MgO	Fe ₂ O ₃	SO ₃	K ₂ O	L.O.I	Color	Density (g/cm ³)	Particle size (nm)
NMM	58.5	5.9	16.55	0.32	2.3	1.43	0.8	14.2	Pale yellow	0.6	10-Aug
CNMM	56.4	3.8	34.37	0.19	1.87	1.58	0.47	1.32	Reddish brown	0.85	4-Feb

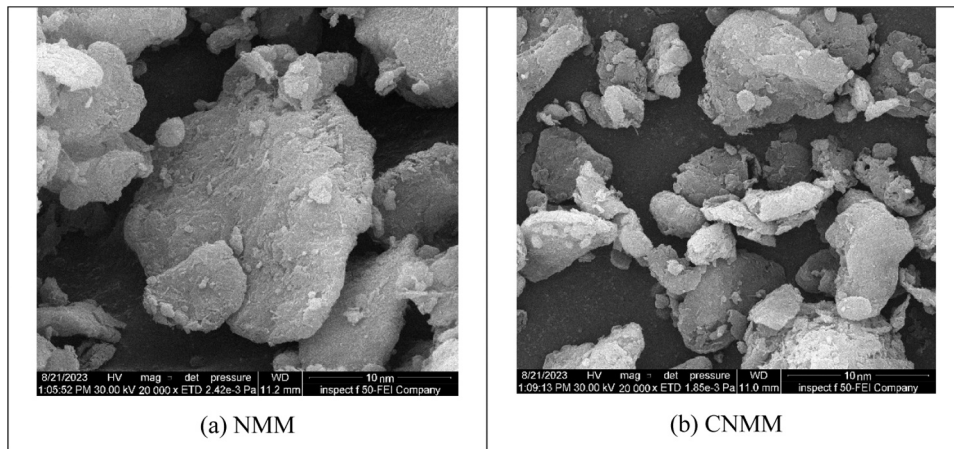


Fig. 2. SEM images of the NMM and CNMM.

3. Nanomaterial addition method and mix preparation

NMM and CNMM were added into asphalt cement by the percentages of weight of the asphalt cement with an increment of 2% from 0% to 10% s. The asphalt cement was firstly heated in an oven of at the temperature of 145 ± 5 °C for 2 h. Adding in the nano clays, the binders were placed on a hotplate and blended using a shear mixer running at 3000 rpm for roughly 45 min.

Preparing the asphalt concrete mixes, aggregates were sieved for the sizes of 19, 12.5, 9.5, 4.75, 2.36, 0.3, and 0.075 mm, for which the part smaller than 0.075 mm were replaced using the limestone filler of the size. The aggregates were recombined in the mixing bowl according to the design specification described in the preceding Section 2.2. These recombined aggregates were continuously mixed on a hot plate for two minutes before put in an oven to be heated for 2 h 150 °C. Prepared asphalt binders were preheated to a temperature of 150–155 °C and added into the heated aggregates. The mixes were then blended rigorously on a hot plate for another two minutes before transferred in an oven set at 140 °C for other 10 min. In the meanwhile, the molds for compaction were given preheating up to 100 °C. Finally, the heated mixes were carefully loaded into the mold and compacted to prepare the specimens for property tests. Each mix had three specimens cast for each test.

4. Experimental tests

4.1. Tests for binders

To assess the stiffening impact of NMM and CNMM on the asphalt binder, penetration and softening point tests were conducted in compliance with ASTM D5 and ASTM D36 standards, respectively, on the binders modified with the dosages of 0, 2, 4, 6, 8, and 10% by weight of asphalt cement. In addition, Storage stability test was also performed to evaluate the efficacy of the mixing procedures following the ASTM D7173 protocol by measuring the disparity between the softening points (ΔT) of the upper and lower part of the samples drawn from a tube, which reflects the uniformity and degree of sedimentation of the nano particles within the asphalt cement matrix. The lower the ΔT value the better the dispersion, blend, suspension of nanoclay particles within the asphalt cement.

4.2. Tests for asphalt concrete mixtures

4.2.1. Marshall properties

Marshall test is to evaluate the resistance to plastic deformation of asphalt concrete (ASTM D6927) and determine the contents of air voids (%AV), voids in mineral aggregates (%VMA) and voids filled by asphalt (%VFA). (ASTM-D2726–04) and the theoretical specific gravity of mixtures derived from uncompacted mixture (ASTM-D2041).

4.2.2. Moisture susceptibility

The moisture susceptibility of the mixtures was evaluated in compliance with ASTM-D-4867. For each mix, six cylindrical specimens were fabricated using the same method as the above Marshall test but the number of compaction blows varies between 48 and 61 on each end of the molds to have the specimens an air void (AV) content of 6–8%. The prepared specimens possessed dimensions of 101.6 mm (4 in.) in diameter and 63 mm (2.5 in.) in height. All the cast specimens in triplicate were divided into two sets, one of which was tested at ambient temperature (25 °C) and labeled as dry or unconditioned, while the other set, labeled as wet or conditioned, was submerged in water of 25 °C and in an airtight container. The specimens in a vacuum pressure of 70kPa or 525 mm Hg was applied on the airtight container for 5 min to ensure the specimens inside to achieve a water saturation level of 55–80%. Subsequently, the conditioned specimens were exposed to a freeze-thaw cycle with exposure to -18 ± 2 °C for 16 h followed by immersion at 60 ± 1 °C for a subsequent 24 h. After these treatments, all specimens in both sets were tested at room temperature (25 °C) for their indirect tensile strength (ITS) and tensile strength ratio (TSR).

4.2.3. Resilient modulus and permanent deformation

Uniaxial repeated load tests were performed on cylindrical specimens of the dimensions, 101.6 mm (4 in.) in diameter and 203.2 mm (8 in.) in height. Tests were performed under two controlled temperature conditions, they were 40 °C (104°F) for evaluating permanent deformation and 20 °C (68°F) for resilient modulus. The compaction of the test specimen was achieved using the double plunger method, where a 29,491 kg (65,000 lb) load was applied by a hydraulic compression machine to each end of the specimen for one minute. Then, the specimen was gently moved to a smooth, flat surface and allowed to cool overnight at room temperature. Subsequently, it was removed from the mold using a hydraulic extractor, labeled, and stored in a bag until ready for testing. The detailed procedure for specimen preparation can be found in another reported work [3].

4.2.4. Fatigue test

Indirect tensile cracking test (IDEAL-CT) was conducted to evaluate fatigue resistance of the asphalt concrete mixes at a temperature between 5 °C and 35 °C upon local climate. Its ascendancy in popularity can be attributed to its straightforward implementation (no instrumentation, cutting, gluing, drilling, or notching of specimens) practicability (minimal training required for routine operation), efficiency (test completion in less than one minute), repeatability (coefficient of variance less than 25%), and low cost of test apparatus. Following the ASTM D 8225, cylindrical specimens, with dimensions of 101.6 mm (4 in.) in height and 63 mm (2.5 in.) in diameter, subjected a consistent vertical load at a rate of 50 mm/min along its diametrical axis, with simultaneous monitoring of both applied load and resultant displacement throughout the test's entirety. In IDEAL-CT test, Marshall specimens are used that compacted to an air void level $7 \pm 0.5\%$ using 48–61 blows at each face of the specimen using Marshall compactor. Testing is conducted at a constant temperature of 20 °C, each test was performed in triplicate and average results were calculated. Fig. 3 depicts a typical load-displacement graph resultant from IDEAL-CT test.

The CT_{index} of asphalt concrete specimen is calculated as per the Eq. (1) below:

$$CT_{index} = \frac{t}{62} \times \frac{i_{75}}{D} \times \frac{G_f}{m_{75}} \times 10^6 \quad (1)$$

The failure energy, G_f , is the area under the curve divided by the specimen's cross-sectional area; the post-peak slope, m_{75} , is the absolute value of the slope of the load-displacement curve at the point where the post-peak load decreases to 75% of the peak load; and the deformation tolerance, i_{75} , is the displacement at 75% of the peak load.

5. Results and discussion

5.1. Physical properties of binders

Figs. 4 and 5 show the results of the consistency test for penetration and susceptibility test for softening point, which indicate that

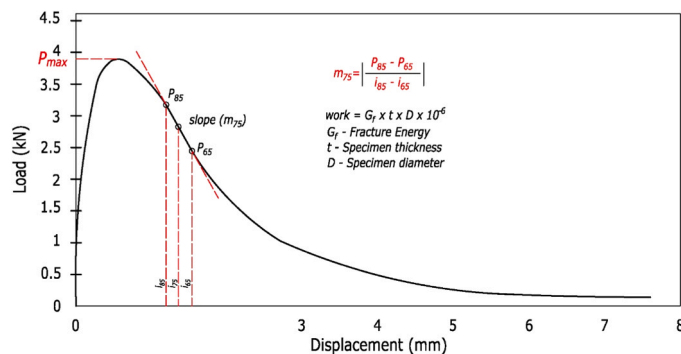


Fig. 3. Typical load-displacement curve in IDEAL-CT test.

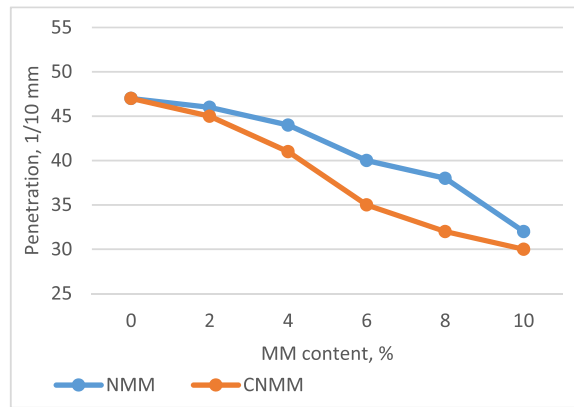


Fig. 4. Penetration test results.

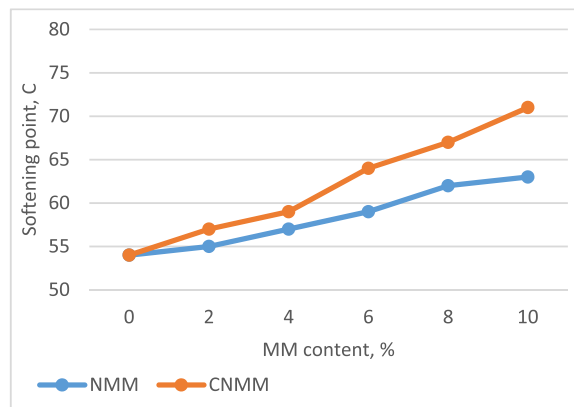


Fig. 5. Softening points test results.

the addition of nanoclays will decrease the penetration value but increase the softening temperature of the modified binders. The increment of NMM from 0% to 10% has led about 31.9% reduction of the penetration value (from 47 to 32). However, using CNMM at the same rates has generated higher decline of approximately 36.2% (from 47 to 30). In contrast, the softening temperature of the NMM asphalt binder has an increment about 16.7% (from 54 °C to 63 °C) when NMM increases from 0% to 10%, and that of the CNMM asphalt binder has a higher increment of 31.5% (from 54 °C to 71 °C) when CNMM increases from 0% to 10%. The more influential effect of the CNMM, compared with NMM, on the penetration value and the softening point of the modified asphalt binder can be attributed to its fragmented structure in the form of smaller particles, and the strong interfacial bond of the asphalt molecules inside the CNMM layers of particles. The obtained results for the stiffening effect of NMM are in agreement with those of [32].

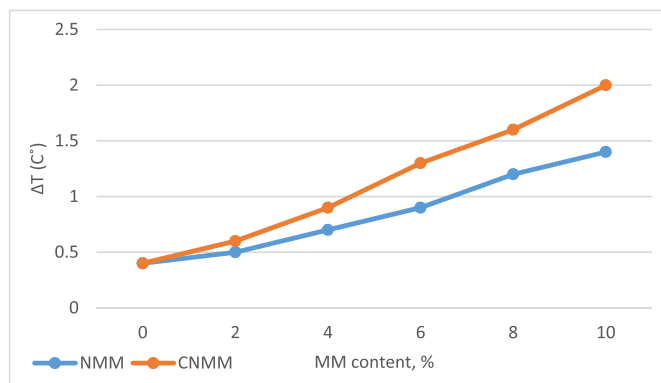
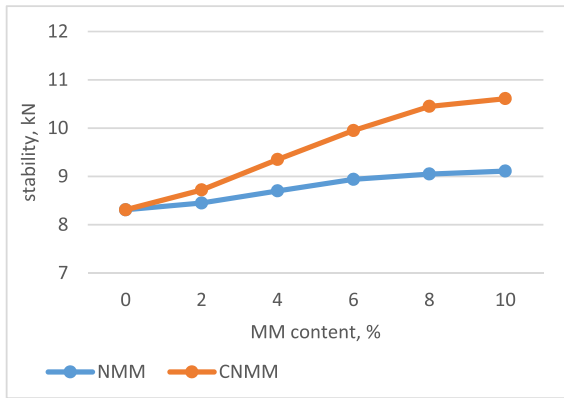


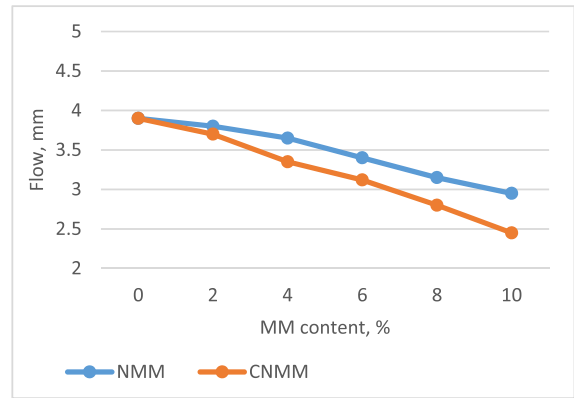
Fig. 6. Storage stability test results.

5.2. Compatibility of additives

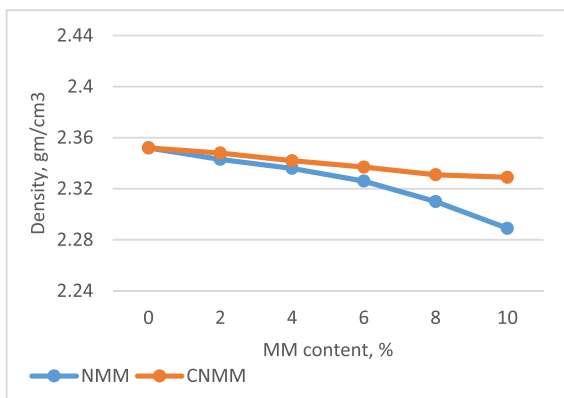
Fig. 6 shows the results of the storage stability test. It can be seen that in general, the ΔT increases with the content of the additives, however, the NMM asphalt binder has a better storage stability than the CNMM asphalt binder with a lower ΔT value. The higher the additive content, the better the stability of the NMM binder than the CNMM binder. The decrease of the stability of CNMM particles in asphalt matrix may be attributed to the higher density of CNMM, which is 0.85 gm/cm^3 , than that of NMM, which is 0.60 gm/cm^3 . The higher density of CNMM is a result of the calcination, which has reduced the moisture and organism content. Although closer to the limit, the ΔT of investigated CNMM concentration range is within the acceptable range of the compatibility with the asphalt binder



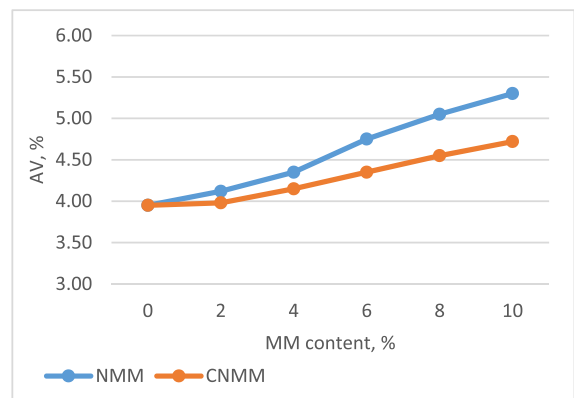
(a) Stability



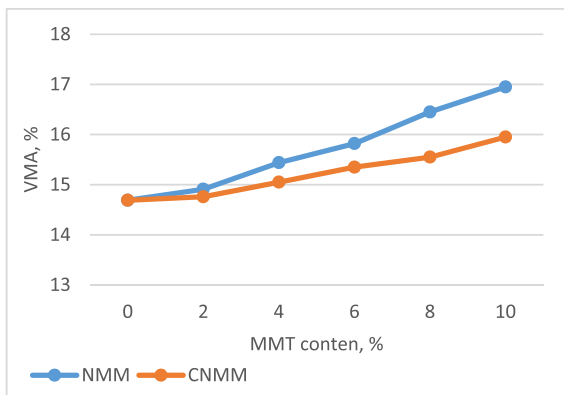
(b) Flow



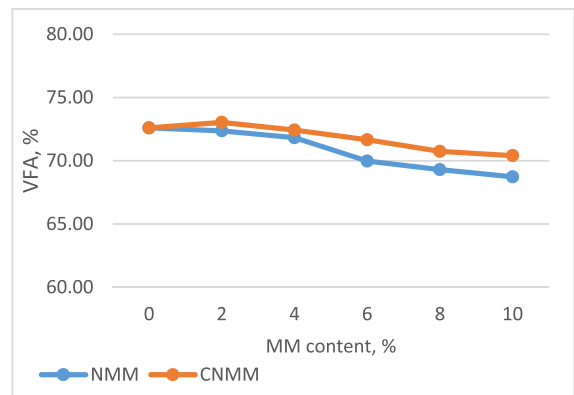
(c) Density



(d) Air Voids



(e) VMA



(f) VFA

Fig. 7. Marshall Properties test results.

(less than 2.2 °C).

5.3. Performance of the modified asphalt concrete mixture

5.3.1. Marshall properties

Fig. 7 gives out the results of the Marshall test. In general, nanoclays show improvement on asphalt stability, flow resistance, increasing the density of binders. The higher the nanoclay content, the higher the air void and the voids in the mineral aggregates, but the lower the voids filled by asphalt. The comparison between the property curves of the NMM and the CNMM asphalt concretes, it can be clearly seen that CNMM demonstrates a better enhancement on the concrete stability and flow resistance than the NMM. The CNMM asphalt concrete also has lower VA and VMA because of a higher density, but higher VFA because of more asphalt binder molecules enter into the interstices inside the layered nano particles. The level of the outperformance of the CNMM than the NMM on all the Marshall properties is increasingly pronounced with the addition increment up to 10%.

5.3.2. Moisture susceptibility results

Figs. 8 and 9 shows the results of the moisture susceptibility tests. In general, the MM enhances the moisture resistance of asphalt concrete. However, the NMM shows the an optimum content at 4%, while the CNMM shows a steady improvement, i.e., the higher the CNMM content the higher the TSR. A reasonable explanation for the results is the calcination has considerably reduced the initial moisture content of the additive, CNMM. The obtained results for the NMM improvement of moisture damage resistance align with those of [24], who noted a peak resistance to moisture damage at a 4% NMM concentration.

5.3.3. Resilient modulus results

Fig. 10 shows that results of resilient modulus test, which presents that both modifiers increasingly enhance the Mr magnitudes as their content increases. Comparing the NMM and CNMM, the latter one demonstrates a better performance. Its improving capacity on the stiffness of asphalt concrete steadily continue to increase with the increment of addition up to 10%, however, in contrast, the improvement using NMM has almost stopped at the rate of 6%. The outperformance of CNMM than NMM can be explained against the SEM analysis images. The CNMM particles present a disruptive fragmented structure, and are in much smaller size. They have a rougher or more irregular surface texture. Such characteristic increases the interfacial friction and the interlock between particles, which helps enhance the stiffness of mixtures.

5.3.4. Permanent deformation results

Fig. 11 gives out the result of the permanent deformation test. The measurements were given a characteristic fitting using a power function, Eq. (2).

$$\epsilon_p = aN^b \quad (2)$$

where, ϵ_p is the permanent strain, N is the number of axial load repetition, a and b are two constants. The fitting results in the form of the solid curves demonstrate that the Eq. (2) has presented a good representation for the permanent deformation characteristic. In the log-log scale, Eq. (2) displaces in a form of linear straight line, for which the parameter $\log(a)$ stands for the interception on the vertical axis $\log(\epsilon_p)$ and the parameter b stands for the slope of the straight line.

Fig. 12 compares the a and b of the fitting curves. It can be seen that the parameter a of the CNMM curves is bigger than that of the NMM curves, while the b of the CNMM curves is smaller than that of the NMM curves. It means that CNMM asphalt concrete could have a larger permanent deformation at the start of loading, but the accumulated permanent deformation is smaller than that of the NMM asphalt concrete after the same number of load cycles. Specifically, compared to NMM mixes, CNMM mixes showcased a substantial 19.17% improvement in slope values at the 10% content level. Moreover, under conditions of 10,000 load repetitions, CNMM

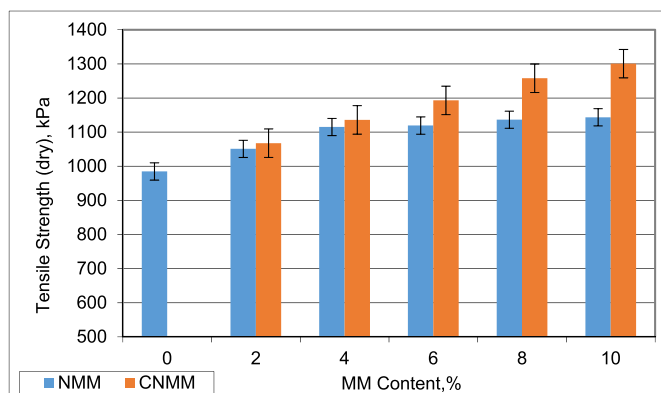


Fig. 8. Effect of modifiers on ITS dry test results.

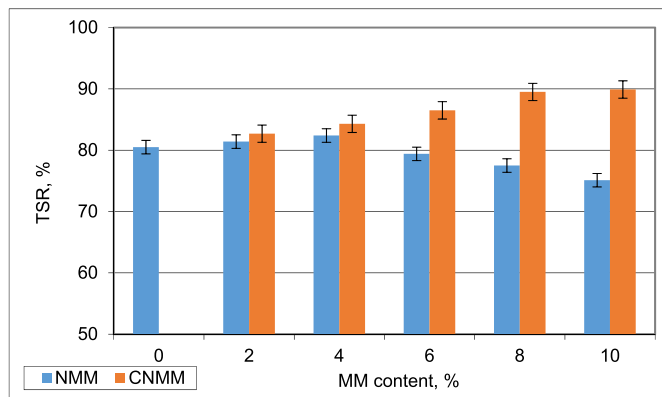


Fig. 9. Effect of modifiers on TSR results.

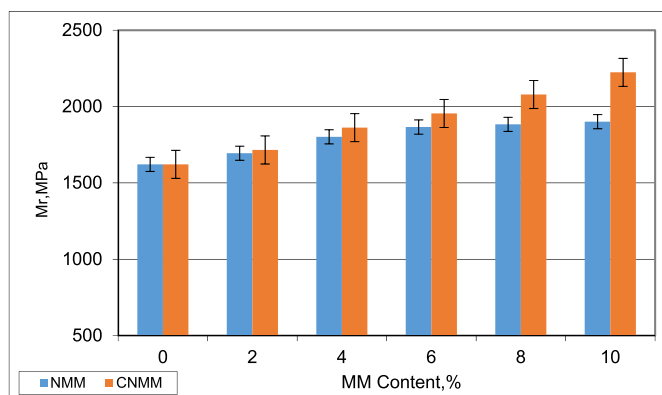


Fig. 10. Effect of modifiers on Mr results.

exhibited a remarkable 5.25% reduction in permanent deformation, further highlighting its superior ability to resist permanent deformation.

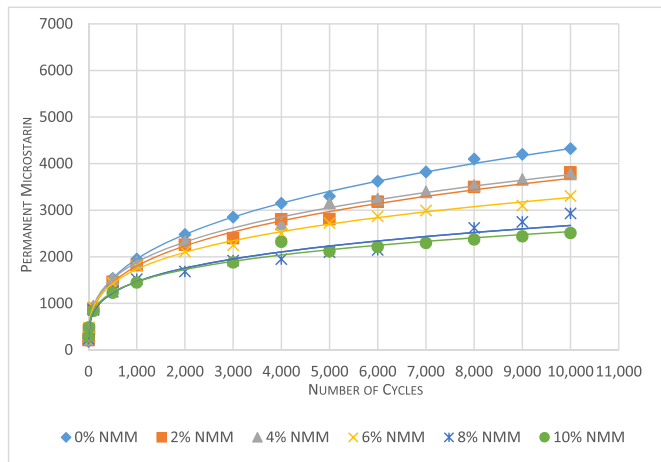
5.3.5. Fatigue cracking results

Based on the data presented in Figs. 13a and 13b, distinct trends emerge for NMM and CNMM. Referring to Fig. 13a for the CTindex results, for NMM, the peak fatigue resistance is identified at the 4% content, with a CTindex of 165. Beyond this, there's a noticeable decline, suggesting an optimal threshold beyond which fatigue resistance decreases. Conversely, CNMM showcases a continuous ascent in CTindex values, signifying its enhanced resistance to fatigue cracking. Notably, the improvement pace is especially pronounced between 0% and 6%, registering a 57.5% enhancement from the baseline of 0%. As the content increases to 10%, there is a 63.33% rise in the CTindex, yet the gradient of improvement tends to level off, implying a reduced incremental benefit beyond the 6% content. Turning to Fig. 13b for the Gf outcomes, CNMM at 6% content realizes a Gf value of 8621j/m². This high value accentuates CNMM's pronounced ability to resist crack initiation, especially when compared to NMM. In conclusion, the combined assessment of CTindex and Gf elucidates the distinctive fatigue resistance attributes of both NMM and CNMM, with CNMM displaying superior resistance, particularly at a 6% content.

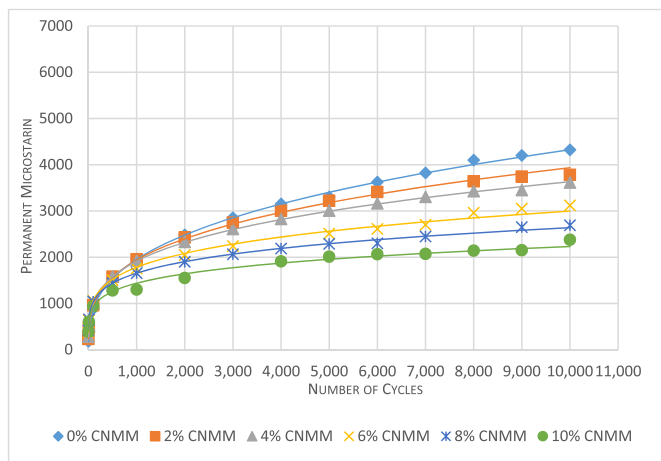
6. Cost analysis

A reference of the local prices for all the raw materials used in this study are listed in Table 5. The total cost of each mix per cubic meter, based on these reference prices, and the corresponding percentage increase in cost compared to the control mix (0% MM content) are presented in Fig. 15.

It's evident that the CNMM modifier results in a rise of cost. The higher the MM content the more costly using CNMM than using NMM. The cost increase rate with the MM content (%) is about 6.6% for CNMM asphalt binder and 4.7% for NMM modified binder. To provide insights into the cost-effectiveness of each type and to conclude the optimum modifier quantity ensuring the best performance enhancements at the most competitive price, a parameter "Gain" is introduced, which is defined as the ratio of the improvement percentage of a specific property of modified binders on the control benchmarks to the increment percentage in cost. Fig. 15 compares the parameter Gain in terms of the Marshall stability, TSR, Mr, ϵ_p at 10,000 load repetitions, and CT index for the CNMM and NMM



(a) NMM



(b) CNMM

Fig. 11. Effect of modifiers on permanent deformation.

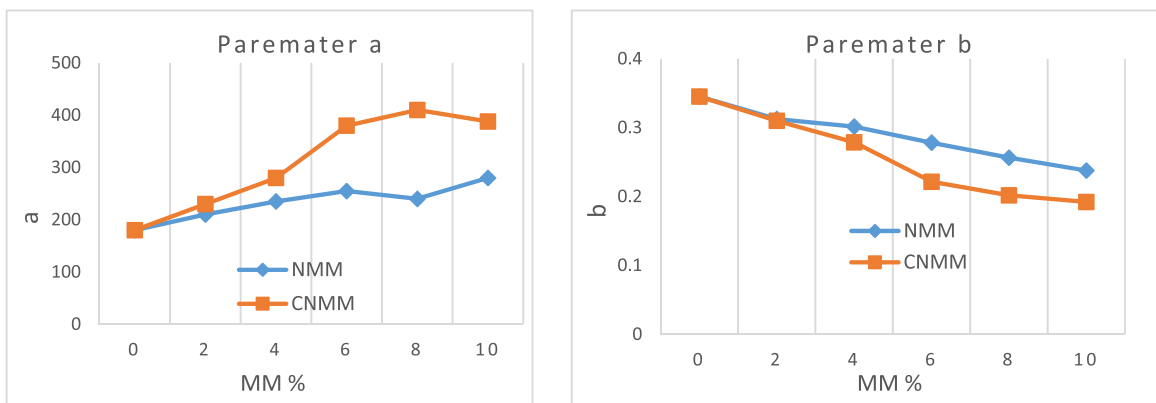
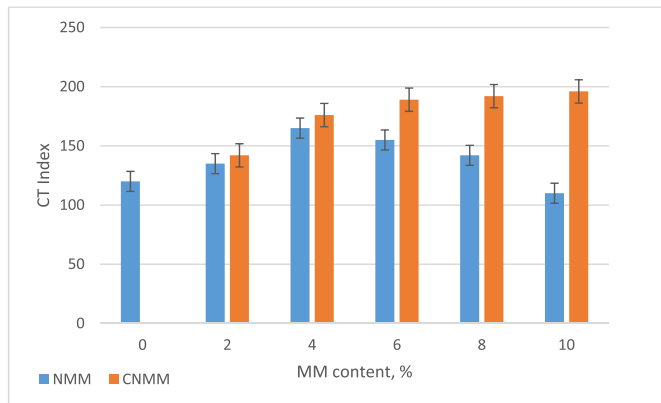
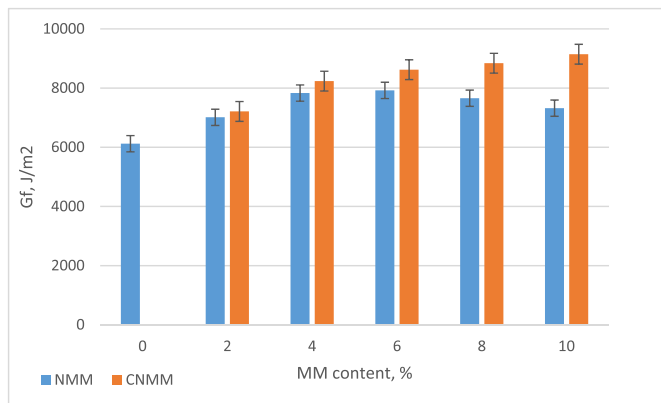


Fig. 12. Effect of modifiers on permanent deformation parameters.



(a) Ct index



(b) fracture energy

Fig. 13. Effect of modifiers on fatigue cracking results.

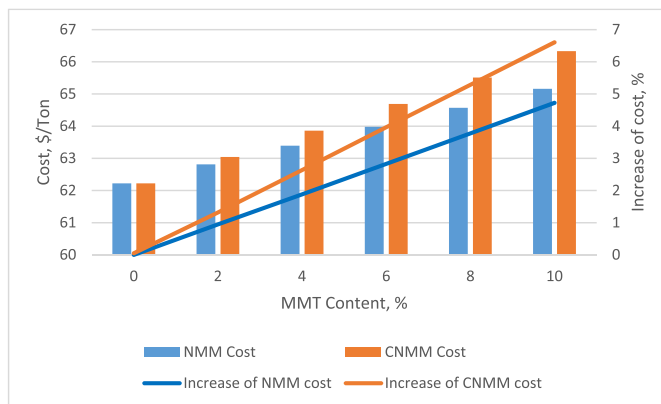


Fig. 14. Mixes cost and percent change in cost.

modification. The diagram indicates that for CNMM 4% addition generates the best Gain for the mechanical properties, Stability, TSR and Mr, but 2% for ϵ_p , and 6% for CT index, while in contrast, for NMM, 4% addition generates the best Gain for TSR, Mr and CT index, 6% for Stability, 2% for ϵ_p .

Table 5
Reference local prices for mix constituents.

Material	Cost
Coarse aggregate	11\$/Ton
Fine aggregate	8.16\$/ Ton
Mineral filler	60\$/ Ton
Asphalt cement	270\$/ Ton
NMM	250\$/ Ton
CNMM	350\$/ Ton

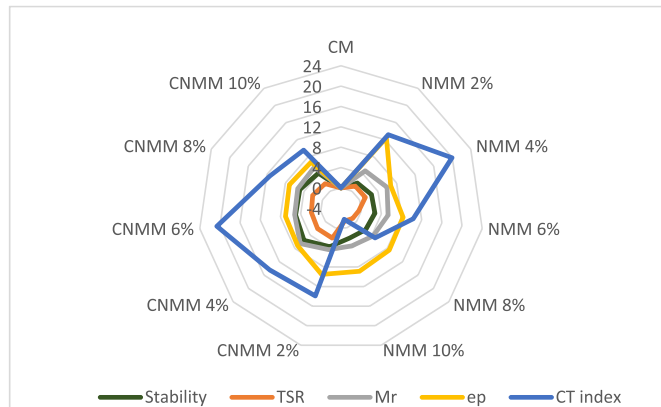


Fig. 15. The comparison of Gain values for different mixes.

7. Conclusions

Based on the experimental tests on both the modified asphalt binders and the concrete mixes using the NMM and CNMM, respectively, the following finds can be concluded:

1. CNMM particles have rougher surface and more irregular shape than NMM particles, which help enhance both physical and chemical adhesion with asphalt binder.
2. CNMM helps enhance the stiffness of binder. At 10% content, the penetration value and softening point are 20% less and 5 °C higher, respectively, in comparison with the use of NMM.
3. CNMM improves the Marshall Stability of mixtures by approximately 15% at 6% content, in comparison with NMM.
4. CNMM presented 32% improvement on ITS at 10% content at normal condition. However, it significantly improves the moisture susceptibility of mixes at 8% content, when the TSR exceeds 80%.
5. CNMM substantially improves the permanent deformation resistance. At 10% content, there is 19.17% improvement in a slope values, which indicates a slowed rate of the accumulated permanent deformation. After 10,000 load repetitions, CNMM mixes showed 5.25% less permanent deformation.
6. At 6% content, CNMM displayed a significant 57.5% improvement on the CTindex and achieved a high Gf value up to 8621j/m², which indicate a higher capacity of fatigue crack resistance, in comparison with NMM.
7. NMM presents the optimum content at around 4%, thereafter its beneficial effect declines rapidly, while the optimum content of CNMM is at around 6%. However, CNMM continues improving capacity beyond the point, but the rate starts to decline.

In summary, for practitioners considering the use of CNMM as an asphalt binder additive modifier, adapting to specific site conditions is essential to optimize pavement performance and cost-effectiveness, as per the findings of this study. However, it's crucial to acknowledge the limitations due to the conclusions being primarily based on laboratory experiments. Further real-world validations are necessary to acquire a comprehensive and robust assessment of CNMM's feasibility and reliability in practical engineering applications. This enhanced validation will help ensure that the application of CNMM as a modifier is both technically sound and practically viable.

Declaration of Competing Interest

The authors declare that there is no conflict of interest regarding the publication of this paper.

Data Availability

Data will be made available on request.

References

- [1] M.E. Abdullah, M.R. Hainin, N.I.M. Yusoff, K.A. Zamhari, N. Hassan, Laboratory evaluation on the characteristics and pollutant emissions of nanoclay and chemical warm mix asphalt modified binders, *Constr. Build. Mater.* 113 (2016) 488–497, <https://doi.org/10.1016/j.conbuildmat.2016.03.068>.
- [3] A.H. Albayati, Performance evaluation of plant produced warm mix asphalt (17264073), *J. Eng.* 24 (5) (2018), <https://doi.org/10.31026/j.eng.2018.05.10>.
- [4] A. Albayati, Y. Wang, J. Haynes, Size effect of hydrated lime on the mechanical performance of asphalt concrete, *Materials* 15 (10) (2022) 3715, <https://doi.org/10.3390/ma15103715>.
- [5] M.H. Ali Hassan, M. El-Gendy, M. El-Refaey, Enhancing the performance of warm asphalt mixes using nano-kaolinite, *J. Al-Azhar Univ. Eng. Sect.* 17 (63) (2022) 469–479, <https://doi.org/10.21608/aej.2022.233742>.
- [6] A.F. Al-Tameemi, Y. Wang, A. Albayati, Experimental study of the performance related properties of asphalt concrete modified with hydrated lime, *J. Mater. Civ. Eng.* 28 (5) (2016), 04015185, [https://doi.org/10.1061/\(ASCE\)MT.1943-5533.0001474](https://doi.org/10.1061/(ASCE)MT.1943-5533.0001474).
- [7] A.F. Al-Tameemi, Y. Wang, A. Albayati, J. Haynes, Moisture susceptibility and fatigue performance of hydrated lime-modified asphalt concrete: Experiment and design application case study, *J. Mater. Civ. Eng.* 31 (4) (2019), 04019019, [https://doi.org/10.1061/\(ASCE\)MT.1943-5533.0002634](https://doi.org/10.1061/(ASCE)MT.1943-5533.0002634).
- [8] M. Ameri, R. Mohammadi, M. Vamegh, M. Molyayem, Evaluation the effects of nanoclay on permanent deformation behavior of stone mastic asphalt mixtures, *Constr. Build. Mater.* 156 (2017) 107–113, <https://doi.org/10.1016/j.conbuildmat.2017.07.055>.
- [9] P.K. Ashish, D. Singh, S. Bohm, Investigation on influence of nanoclay addition on rheological performance of asphalt binder, *Road. Mater. Pavement Des.* 18 (5) (2017) 1007–1026, <https://doi.org/10.1080/14680629.2016.1201522>.
- [10] A.M. Azam, S.M. El-Badawy, R.M. Alabasse, Evaluation of asphalt mixtures modified with polymer and wax, *Innov. Infrastruct. Solut.* 4 (2019), 43, <https://doi.org/10.1007/s41062-019-0230-3>.
- [11] S.A. Bagshaw, T. Kemmitt, M. Waterland, S. Brooke, Effect of blending conditions on nano-clay bitumen nanocomposite properties, *Road. Mater. Pavement Des.* 20 (8) (2019) 1735–1756, <https://doi.org/10.1080/14680629.2018.1468802>.
- [12] K.A. Boateng, Y.A. Tuffour, S. Agyeman, F. Boadu, Potential improvements in montmorillonite-nanoclay-modified Cold-Mix Asphalt, *Case Stud. Constr. Mater.* 17 (2022), e01331, <https://doi.org/10.1016/j.cscm.2022.e01331>.
- [14] A. El Badawy A. Rahim Evaluation of Nanoclay Additives for Improving Resistance to Moisture Damage in Hot Mix [Summary] (No. Project 2151). San Jose State University. College of Business. Mineta Transportation Institute. <https://doi.org/10.31979/mti.2023.2151>.
- [15] Eman Mousa, Sherif El-Badawy, Abdelhalim Azam, Evaluation of reclaimed asphalt pavement as base/subbase material in Egypt, *Transp. Geotech.* Volume 26 (2021), 100414, <https://doi.org/10.1016/j.trgeo.2020.100414>.
- [16] H. Ezzat, S. El-Badawy, A. Gabr, E.S.I. Zaki, T. Breakah, Evaluation of asphalt binders modified with nanoclay and nanosilica, *Procedia Eng.* 143 (2016) 1260–1267, <https://doi.org/10.1016/j.proeng.2016.06.119>.
- [17] C. Fang, R. Yu, S. Liu, Y. Li, Nanomaterials applied in asphalt modification: a review, *J. Mater. Sci. Technol.* 29 (7) (2013) 589–594, <https://doi.org/10.1016/j.jmst.2013.04.008>.
- [18] H. Fida, G. Zhang, S. Guo, A. Naeem, Heterogeneous Fenton degradation of organic dyes in batch and fixed bed using La-Fe montmorillonite as catalyst, *J. Colloid Interface Sci.* 490 (2017) 859–868, <https://doi.org/10.1016/j.jcis.2016.11.085>.
- [19] T. Gehlot, Use of nano-clay in asphalt binder modification, *J. Mech. Civ. Eng.* 15 (2018) 25–30.
- [20] P. Ghoddousi, M. Zareechian, A.A.S. Javid, A.H. Korayem, Microstructural study and surface properties of concrete pavements containing nanoparticles, *Constr. Build. Mater.* 262 (2020), 120103, <https://doi.org/10.1016/j.conbuildmat.2020.120103>.
- [21] G.H. Hamed, F. Moghadas Nejad, K. Oveisi, Investigating the effects of using nanomaterials on moisture damage of HMA, *Road. Mater. Pavement Des.* 16 (3) (2015) 536–552, <https://doi.org/10.1080/14680629.2015.1020850>.
- [22] I. Hannus, I. Pálkó, K. Lázár, J.B. Nagy, I. Kiricsi, The chemical state of Sn in Sn-montmorillonite; a multinuclear MAS NMR and ¹¹⁹Sn Mössbauer spectroscopic study, *J. Mol. Struct.* 349 (1995) 179–182, [https://doi.org/10.1016/0022-2860\(95\)08738-H](https://doi.org/10.1016/0022-2860(95)08738-H).
- [23] Z. Hossain, M. Zaman, M.C. Saha, T. Hawa, Evaluation of moisture susceptibility and healing properties of nanoclay-modified asphalt binders, *IFCEE 2015* (2015) 339–348, <https://doi.org/10.1061/9780784479087.034>.
- [24] Saif Al-din Majid Ismael, Mohammed Qadir Ismael, Moisture susceptibility of asphalt concrete pavement modified by nanoclay additive, *Civ. Eng. J.* 5 (12) (2019) 2535–2553, <https://doi.org/10.28991/cej-2019-03091431>.
- [25] J. Jin, B. Chen, L. Liu, R. Liu, G. Qian, H. Wei, J. Zheng, A study on modified bitumen with metal doped nano-TiO₂ pillared montmorillonite, *Materials* 12 (12) (2019) 1910, <https://doi.org/10.3390/ma12121910>.
- [26] J. Jin, T. Xiao, Y. Tan, J. Zheng, R. Liu, G. Qian, J. Zhang, Effects of TiO₂ pillared montmorillonite nanocomposites on the properties of asphalt with exhaust catalytic capacity, *J. Clean. Prod.* 205 (2018) 339–349, <https://doi.org/10.1016/j.jclepro.2018.08.251>.
- [27] H.H. Joni, H.H. Zghair, A.A. Mohammed, Rutting parameters of modified asphalt binder with micro and nano-size of metakaolin powder, *J. Eng. Sci. Technol.* 15 (5) (2020) 3465–3480.
- [28] A. Juraidah, P.J. Ramadhansyah, M.K. Azman, C.M. Nurulain, M.M. Naquiddin, A.H. Norhidayah, M. Nordiana, Performance of Nano kaolin clay as modified binder in porous asphalt mixture (February), in: *In IOP Conference Series: Earth and Environmental Science*, Vol. 244, IOP Publishing, 2019, 012036, <https://doi.org/10.1088/1755-1315/244/1/012036> (February).
- [29] Y.C. Ke, P. Stroeve, Polymer-layered silicate and silica nanocomposites, Elsevier, 2005, <https://doi.org/10.1016/B978-044451570-4/50004-5>.
- [30] Khodary, F. (2015). Longer fatigue life for asphalt pavement using (SBS@ clay) nanocomposite. *International journal of current engineering and technology*, 5 (2).
- [31] R. Li, F. Xiao, S. Amirhanian, Z. You, J. Huang, Developments of nano materials and technologies on asphalt materials-a review, *Constr. Build. Mater.* 143 (2017) 633–648, <https://doi.org/10.1016/j.conbuildmat.2017.03.158>.
- [32] Xian Li, et al., Effect of montmorillonite modification on resistance to thermal oxidation aging of asphalt binder, *Case Stud. Constr. Mater.* 16 (2022), e00971, <https://doi.org/10.1016/j.cscm.2022.e00971>.
- [33] A. Mansourian, A.R. Goahri, F.K. Khosrowshahi, Performance evaluation of asphalt binder modified with EVA/HDPE/nanoclay based on linear and non-linear viscoelastic behaviors, *Constr. Build. Mater.* 208 (2019) 554–563, <https://doi.org/10.1016/j.conbuildmat.2019.03.065>.
- [34] F.C. Martinho, J.P.S. Farinha, An overview of the use of nanoclay modified bitumen in asphalt mixtures for enhanced flexible pavement performances, *Road. Mater. Pavement Des.* 20 (3) (2019) 671–701, <https://doi.org/10.1080/14680629.2017.1408482>.
- [35] A.R. Moeini, A. Badiei, A.M. Rashidi, Effect of nanosilica morphology on modification of asphalt binder, *Road. Mater. Pavement Des.* 21 (8) (2020) 2230–2246, <https://doi.org/10.1080/14680629.2019.1602072>.
- [36] Mohamed G. Arab, Majed Alzara, Waleed Zeiada, Maher Omar, Abdelhalim Azam, Combined effect of compaction level and matric suction conditions on flexible pavement performance using construction and demolition waste, *Constr. Build. Mater.* Volume 261 (2020), 119792, <https://doi.org/10.1016/j.conbuildmat.2020.119792>.
- [37] M. Mohammadiroudbari, A. Tavakoli, M.K.R. Aghjeh, M. Rahi, Effect of nanoclay on the morphology of polyethylene modified bitumen, *Constr. Build. Mater.* 116 (2016) 245–251, <https://doi.org/10.1016/j.conbuildmat.2016.04.098>.
- [38] E. Mousa, S. El-Badawy, A. Azam, Effect of reclaimed asphalt pavement in granular base layers on predicted pavement performance in Egypt, *Innov. Infrastruct. Solut.* 5 (2020), 57, <https://doi.org/10.1007/s41062-020-00301-2>.

- [39] SCRB/R9. (2003). General Specification for Roads and Bridges, Section R/9, Hot-Mix Asphalt Concrete Pavement, Revised Edition. State Corporation of Roads and Bridges, Ministry of Housing and Construction, Republic of Iraq.
- [40] G. Shafabakhsh, M. Aliakbari Bidokhti, H. Divandari, Investigating the rutting behavior of modified bitumen with SBS/MgO nanocomposite, *J. Transp. Infrastruct. Eng.* 6 (3) (2020) 31–46.
- [41] E.A. Siddig, C.P. Feng, L.Y. Ming, Effects of ethylene vinyl acetate and nanoclay additions on high-temperature performance of asphalt binders, *Constr. Build. Mater.* 169 (2018) 276–282, <https://doi.org/10.1016/j.conbuildmat.2018.03.012>.
- [42] M. Sukhija, N. Saboo, Influence of nanoclay in viscosity graded asphalt binder at different test temperatures, *Adv. Mater. Pavement Perform. Predict. II* (2020) 101–104, <https://doi.org/10.1201/9781003027362-25>.
- [43] E.W. Tarbay, A.M. Azam, S.M. El-Badawy, Waste materials and by-products as mineral fillers in asphalt mixtures, *Innov. Infrastruct. Solut.* 4 (2019), 5, <https://doi.org/10.1007/s41062-018-0190-z>.
- [45] Y. Wang, R.H. Latief, H. Al-Mosawe, H.K. Mohammad, A. Albayati, J. Haynes, Influence of iron filing waste on the performance of warm mix asphalt, *Sustainability* 13 (24) (2021) 13828, <https://doi.org/10.3390/su132413828>.
- [46] H. Yao, Z. You, L. Li, S.W. Goh, C.H. Lee, Y.K. Yap, X. Shi, Rheological properties and chemical analysis of nanoclay and carbon microfiber modified asphalt with Fourier transform infrared spectroscopy, *Constr. Build. Mater.* 38 (2013) 327–337, <https://doi.org/10.1016/j.conbuildmat.2012.08.004>.
- [47] Z. You, J. Mills-Beale, J.M. Foley, S. Roy, G.M. Odegard, Q. Dai, S.W. Goh, Nanoclay-modified asphalt materials: preparation and characterization, *Constr. Build. Mater.* 25 (2) (2011) 1072–1078, <https://doi.org/10.1016/j.conbuildmat.2010.06.070>.
- [48] S. Zapién-Castillo, J.L. Rivera-Armenta, M.Y. Chávez-Cinco, B.A. Salazar-Cruz, A.M. Mendoza-Martínez, Physical and rheological properties of asphalt modified with SEBS/montmorillonite nanocomposite, *Constr. Build. Mater.* 106 (2016) 349–356, <https://doi.org/10.1016/j.conbuildmat.2015.12.099>.